# Filamin A Is Essential for Active Cell Stiffening but not Passive Stiffening under External Force

K. E. Kasza,[†] F. Nakamura,[§] S. Hu,[¶] P. Kollmannsberger,[‖] N. Bonakdar,[‖] B. Fabry,[‖] T. P. Stossel,[§] N. Wang,[¶**] and D. A. Weitz[†‡*]

[†]School of Engineering and Applied Sciences, and [‡]Department of Physics, Harvard University, Cambridge, Massachusetts; [§]Translational Medicine Division, Brigham and Women's Hospital, Department of Medicine, Harvard Medical School, and [¶]Department of Environmental Health, Harvard School of Public Health, Boston, Massachusetts; [‖]Center for Medical Physics and Technology, Department of Physics, University of Erlangen-Nuremberg, Erlangen, Germany; and [**]Department of Mechanical Science and Engineering, University of Illinois at Urbana-Champaign, Urbana, Illinois

ABSTRACT The material properties of a cell determine how mechanical forces are transmitted through and sensed by that cell. Some types of cells stiffen passively under large external forces, but they can also alter their own stiffness in response to the local mechanical environment or biochemical cues. Here we show that the actin-binding protein filamin A is essential for the active stiffening of cells plated on collagen-coated substrates. This appears to be due to a diminished capability to build up large internal contractile stresses in the absence of filamin A. To show this, we compare the material properties and contractility of two human melanoma cell lines that differ in filamin A expression. The filamin A-deficient M2 cells are softer than the filamin A-replete A7 cells, and exert much smaller contractile stresses on the substratum, even though the M2 cells have similar levels of phosphorylated myosin II light chain and only somewhat diminished adhesion strength. In contrast to A7 cells, the stiffness and contractility of M2 cells are insensitive to either myosin-inhibiting drugs or the stiffness of the substratum. Surprisingly, however, filamin A is not required for passive stiffening under large external forces.

## INTRODUCTION

A cell is a material that has both elastic and viscous properties (1–4) that determine its ability to maintain a stable shape, deform, or remodel. A cell's material properties also govern the way in which mechanical signals, which are critical to cell function and survival, propagate through and are sensed by the cell (5–7). The material properties of a cell are quite unusual in comparison with those of more common materials. For instance, the stiffness of a cell is highly nonlinear and increases dramatically when large external forces are applied (8,9). Unlike a traditional inert material, a cell can actively generate internal contractile tension to pull on its substratum or on neighboring cells (10,11). This active control of internal tension allows the cell to tune its own stiffness (8,12). This unusual elasticity is thought to be largely determined by the actin cytoskeleton, a biopolymer network composed of filamentous actin (F-actin) and associated regulatory, motor, and cross-linking proteins. These binding proteins organize F-actin into the networks and bundles that ultimately determine the material properties of the cytoskeleton. Due to the complexity of cells, determining the precise physical and molecular mechanisms underlying cell elasticity has proven difficult. Nonetheless, a more quantitative model of cell material properties is a necessary step toward gaining a more complete understanding of cell mechanics and mechanotransduction.

Experimental and theoretical investigations of reconstituted cytoskeletal networks in vitro, where the molecular components can be precisely controlled, have been particularly useful in elucidating the physical mechanisms underlying the material properties of biopolymer networks that are similar to those found in cells (13,14). For example, the origins of linear and nonlinear elasticity in very simple cross-linked actin networks have been shown to be entropic in nature and arise from single-filament properties, and are very well described by theoretical models (15). The physical origins of elasticity in more complicated systems, which better mimic the networks within cells, are currently being investigated (16,17). In these cases, even though a fully quantitative theoretical model is still lacking, the in vitro systems can nonetheless provide significant insight into design principles that may be at work in the cell. In one remarkable example, it was found that the unusual elasticity of cells can be reconstituted in a minimal in vitro cytoskeleton formed with purified F-actin, processive assemblies of myosin II, and the actin cross-linking protein filamin A (G. H. Koenderink, unpublished). As in cells, the stiffness of these gels increases with either internal tension generated by myosin (G. H. Koenderink, unpublished) or stress applied externally (16). Without cross-linking of F-actin by filamin A and strong adhesion of the gel at the boundaries, the stresses generated by myosin will quickly relax as actin filaments rearrange or as the gel pulls away from the boundaries. In this in vitro system, it is the buildup of large internal tension that is necessary for stiffening of the biopolymer network.

Within the cell, filamin A cross-links F-actin into orthogonal networks in the cortex (18). It also binds some integrins,

*Submitted October 19, 2008, and accepted for publication February 18, 2009.*

*Correspondence: weitz@seas.harvard.edu

Editor: Reinhard Lipowsky.



0006-3495/09/05/4326/10 $2.00

doi: 10.1016/j.bpj.2009.02.035

providing a link between the actin cytoskeleton and the cell membrane (19,20). Thus, filamin A is a good candidate for involvement in the processes by which internal and external mechanical stress affect cell stiffness. Indeed, filamin A is involved in a number of mechanical cell processes, including cell motility, membrane stability, and mechanoprotection (21–23). However, filamin's contribution to the material properties of the cell remains unclear. There are differing reports regarding the contribution of filamin A to the stiffness of cells, with some finding that filamin A increases cell stiffness by 200–400% (21,24) and others finding an increase of <30% (25). Thus far, filamin's contribution to the stiffening of cells under internal and external stress has not been systematically investigated. A better understanding of the role of filamin A in cell mechanics and of the extent to which an analogy can be made between the material properties of cells and in vitro biopolymer systems, where the physical mechanisms underlying the relationship between stress and stiffness are more easily unraveled, will be an important step toward achieving a more quantitative model of cell mechanics and mechanotransduction.

In this article, we investigate the role of filamin A in determining cell material properties, with a focus on its involvement in the processes by which mechanical stress, both internal and external, affect cell stiffness. We find that loss of filamin A is associated with a strong decrease in internal contractile tension and, as a result, leads to softer cells that do not appear to actively tune their own stiffness. Surprisingly, filamin A is not required for the stiffening of cells under large external stresses, perhaps because of redundancy between different cytoskeletal networks. Our results are consistent with the picture that, as in the in vitro actin-filamin-myosin system, filamin A is essential for the buildup of internal tension within the actin cytoskeleton that leads to stiffening, although the cellular mechanisms underlying this tension buildup are more complex.

## MATERIALS AND METHODS

### Cell culture

M2 human melanoma cells, which do not express filamin A, and A7 cells derived from M2 cells but stably expressing roughly wild-type levels of filamin A after transfection of filamin A cDNA (21) show no difference in the amounts of $\alpha$-actinin (21) or the ARP2/3 complex (18), but we cannot entirely exclude the possibility of differences in other actin-binding proteins. In this study, cells are cultured at 37°C and 5% $CO_2$ in minimum essential medium (Mediatech, Manassas, VA) supplemented with 8% newborn calf serum (Invitrogen, Carlsbad, CA) and 2% fetal calf serum (Invitrogen). Cells are plated on substrates and allowed to grow for 24 h before measurements, unless otherwise noted. For all measurements, cells are subconfluent. To assess the contribution of myosin II generated contractile stresses to cell material properties, blebbistatin (Toronto Research Chemicals, North York, Canada), a specific inhibitor of myosin II activity that keeps myosin II in a weakly bound state to *F*-actin (26) is dissolved in DMSO and added to media at a 50 $\mu$M final concentration. The Rho-associated kinase inhibitor Y-27632 (BIOMOL, Plymouth Meeting, PA) is dissolved in water and added to the media at a final concentration of 10 $\mu$M.

### Preparation of substrates

Polyacrylamide gel substrates are prepared according to the procedure described by Pelham and Wang (27) on 35 mm glass-bottomed culture dishes (MatTek, Ashland, MA). Briefly, the glass is aminosilanized to allow for polyacrylamide attachment. Gel stiffness is varied over 2 orders of magnitude by controlling the concentration of the cross-link bis-acrylamide (Bio-Rad, Hercules, CA) from 0.04% to 0.2% at acrylamide (Bio-Rad) concentrations of 3%, 5%, and 7.5%. For traction measurements, a small volume of 200 nm red latex particles (Invitrogen) is added to the solution to act as a marker of gel deformation. The solution is polymerized on the aminosilanized coverslip by the addition of ammonium persulfate and *n*,*n*,*n*′,*n*′-tetramethylethylenediamine (TEMED). The polymerizing gel is covered with a second unmodified coverslip and inverted to create a flat gel surface toward which the tracer particles settle. After polymerization is complete, the top coverslip is removed and collagen I (Vitrogen; Cohesion Tech, Palo Alto, CA) at 0.1 mg/mL in solution is chemically cross-linked to the gel surface using sulfo-SANPAH (Pierce Biotechnology, Rockford, IL). Collagen attachment and uniformity is confirmed using fluorescent collagen-fluorescein (Elastin Products, Owensville, MO). Comparison with known amounts of fluorescent collagen dried on aminosilanized coverslips allows calibration of the collagen surface density to be ~250–650 ng/cm$^2$ for the gels used in this study (28). Gel thickness is 70–100 $\mu$m as determined by microscopy. The elastic shear modulus $G'$ of macroscopic samples of the polyacrylamide gels is characterized in a rheometer (AR-G2; TA Instruments, New Castle, DE). $G'$ is related to the Young's modulus $E$, reported in this work, by the Poisson ratio, which is taken to be 0.48. Recent work shows that polyacrylamide bulk moduli measured in this way are consistent with atomic force microscopy indentation measurements of polyacrylamide gel substrates (28).

### Confocal microscopy of live and fixed cells

Cells for confocal imaging are plated on glass coverslips or polyacrylamide gel substrates and allowed to grow for 2–24 h. The cells are rinsed with PBS, fixed in 4% formaldehyde (Polysciences, Warrington, PA) in PBS for 20 min, permeabilized with 0.1% Triton-X-100 in PBS for 5 min, blocked with 1% BSA in PBS, incubated with 1 $\mu$g/mL Alexa-488 phalloidin (Invitrogen) and 1% BSA in PBS for 20 min, mounted according to the manufacturer's instructions (SlowFade AntiFade Kit; Invitrogen), and sealed. Live cells are fluorescently labeled (CellTracker Green CMFDA; Invitrogen) according to the manufacturer's instructions. The cells are imaged and sectioned at 100 nm intervals using excitation from the 488 nm line of an argon laser and either a 63×, 1.2 NA water immersion objective or a 100×, 1.4 NA oil immersion objective on a laser scanning confocal microscope (Leica TCS SP5, Wetzlar, Germany).

### Traction force microscopy

Cell contractility is measured using the traction force microscopy (TFM) technique according to previously described methods (11,29,30). Cells are plated sparsely and grown on collagen-coated polyacrylamide substrates. The dish is mounted on a heated microscope stage to maintain 37°C. A phase contrast image is taken to record cell shape, and a fluorescence image of the particles embedded in the gel just below the cell's basal surface is taken to record gel deformation. After the cell is detached from the gel using trypsin-EDTA, a second fluorescence image of the particles in the unstressed gel is taken. Images are recorded on a CCD camera (Andor iXon, Belfast, Northern Ireland) with an image size of 512 × 512 pixels and a pixel size of 450 nm. Displacement fields due to cell tractions are determined using an image correlation method (30), and tractions are determined by means of the Fourier transform traction cytometry technique (29) using a software package kindly provided by Iva Tolic-Norrelykke. For each traction field, the prestress and net contractile moments are calculated as described previously (29), and both measures of cell contractility display the same qualitative trends. Ten to 30 cells of each type are averaged for each condition. We

confirm that addition of trypsin-EDTA does not induce a background expansion or contraction of the gel.

## Magnetic twisting cytometry

Cell material properties are probed by magnetic twisting cytometry (MTC) (2). Cells are plated sparsely on collagen-coated polyacrylamide gels or glass coverslips and allowed to grow for 24 h, unless otherwise noted. For blebbistatin measurements, cells are treated with the drug for 20 min before measurement. Then 4.5-$\mu$m ferromagnetic beads coated with RGD (Arg-Gly-Asp) peptide, which binds specifically to integrins on the cell surface, are incubated with the cells for 15 min. The integrin-bound bead is partially engulfed by the cell, and actin is recruited locally, allowing direct coupling to the actin cytoskeleton. Unbound beads are gently washed away, leaving one or two beads per cell. The dish is mounted on a heated microscope stage to maintain 37°C. Beads in the dish are magnetized by a strong, horizontal magnetic field and then twisted by an oscillatory vertical magnetic field at frequencies of $\omega = 0.6$–2000 rad/s and amplitudes of 25–50 Gauss, corresponding to torques per unit bead volume of $T = 13$–27 Pa. Beads are imaged by bright-field microscopy using a 10× objective. The motions of hundreds of beads in a field of view are recorded with a CCD camera (Hamamatsu C4742-95-12ERG) mounted on an inverted microscope (Leica DM IRE2), and the beads' positions are determined in real time with better than 10 nm accuracy by means of an intensity-weighted center-of-mass algorithm. Beads that are clustered or not attached to a cell are not included in analysis. Typically, the amplitude of bead displacement, $d$, is ~100 nm, which is small enough for $d$ to be linearly related to $T$.

For each bead, we calculate $d$ and the phase lag, $\delta$, of the lateral displacement. From $T$, $d$, and a geometrical factor, $\alpha$, we determine the magnitude of the complex modulus, $|G^*| = \alpha\, T/d$ (2,31), which characterizes overall cell stiffness. $|G^*|$ is log-normally distributed in the population, so we report the geometric mean and standard deviation (SD) for hundreds of cells under each condition. $\delta$ characterizes how solid-like or fluid-like the material is ($\delta = 0$ for an elastic solid, and $\delta = \pi/2$ for a fluid), and is normally distributed in the cell population. The elastic modulus is given by $G' = |G^*|\cos(\delta)$, the viscous modulus by $G'' = |G^*|\sin(\delta)$, and the ratio of elastic to viscous contributions by $G''/G' = tan(\delta)$. Unless otherwise noted, the material properties are reported at $\omega = 5$ rad/s.

To report the viscoelastic moduli, it is necessary to measure the bead-cell contact area and determine $\alpha$ for the M2 and A7 cells. The geometry is characterized with confocal fluorescence microscopy of either labeled live cells or fixed and stained cells. For both cell types, beads are embedded ~50% in the cell (data not shown), so that the same value of $\alpha$ is used. We cannot account for possible effects arising from differences in bead-cell or integrin-cytoskeletal adhesion, but these MTC results are consistent with independent measurements of the same cell lines by atomic force microscopy indentation, for which adhesion contributes quite differently (32). Because bead twisting induces nonuniform stresses and strains in the cell, a model is used to estimate $\alpha$ for the measured geometry (31). Typical stresses are of order 10 Pa, and cell stiffnesses are of order 100 Pa. These measurements reflect properties at the length scale of the bead, which is much larger than cytoskeletal structures but still smaller than the whole cell.

## Magnetic tweezers

Magnetic tweezers are employed to measure the nonlinear mechanical response of single cells (33) grown on 35 mm plastic culture dishes (Nunc, Roskilde, Denmark). Superparamagnetic 4.5 $\mu$m beads (Dynabeads M-450; Invitrogen) coated with human fibronectin (Roche, Basel, Switzerland) are added to the cells ($2 \times 10^5$ beads/dish) and allowed to bind for 30 min. Unbound beads are washed away and the dish is placed on a heated microscope stage. Only cells with a single bead attached are selected. The tip of the magnetic tweezer is placed 20–30 $\mu$m from the bead and a stepwise increasing force of 0.5–10 nN is applied. Bright-field images of the cell, the bead, and the needle tip are taken by a CCD camera (ORCA ER Hamamatsu) at a rate of 40 frames per second at 40× magnification. Bead positions are tracked in real time using an intensity-weighted center-of-mass algorithm. The bead displacement in response to a staircase-like force is equivalent to a superposition of creep measurements. By applying the fit procedure described by Mierke et al. (33), we obtain a value for differential creep compliance or inverse stiffness for every force level and every bead. This stiffness has units of force per displacement and can be related to the modulus by a geometrical factor, which we have not determined. Cell stiffnesses are of order 1 nN/$\mu$m, and from an assumed geometry we estimate that typical stresses rise from 30 to 600 Pa and moduli increase from ~100 to 1000 Pa. To obtain the average response of a cell line, the geometric mean of the log-normally distributed differential stiffness values for every force, averaged over all beads that remain attached to the cell throughout the measurement, is computed.

## Cell adhesion

The spinning disk method as described by Boettiger (34) is modified to run in a commercial stress-controlled rheometer (AR-G2; TA Instruments). Cells are grown sparsely on 22 mm circular glass coverslips that are coated with a solution of 10 $\mu$g/mL collagen I and blocked with BSA (34). The coverslips are inverted and mounted to the rheometer top plate with vacuum grease. With care taken to avoid any drying, this plate is then gently lowered into a 5% solution of dextran (Sigma-Aldrich) in PBS (34), which is contained in a large petri dish attached to the rheometer bottom plate. The coverslip is 3 cm from the bottom of the petri dish and 4 cm from the sides. The rheometer top plate is spun at 175 rad/s for 4 min. In this geometry, fluid shear stresses on the apical surfaces of cells increase linearly with distance from the center of the coverslip, $r$. The coverslip is removed, the cells fixed, and the F-actin stained with fluorescent phalloidin (Invitrogen). The whole area of the coverslip is imaged with a fluorescence stereomicroscope. Relative cell density as a function of $r$ is assessed by means of a radial average of fluorescence intensity. Data are fit by a sigmoidal curve, and the relative adhesion strength of the cells is determined by comparing the radii at which cell density is decreased by half. Shear stresses as a function of $r$ may be calculated as described previously (34); here, they are ~10–50 Pa.

## Western blots

Cells are grown on collagen I-coated substrates, rinsed with PBS, lysed and solubilized in SDS sample buffer, and then heated to 95°C for 5 min. The proteins are separated on a NuPAGE Novex 4–12% Bis-Tris Gel (Invitrogen), followed by Western blotting using an anti-phospho-myosin light chain ($pSer^{19}$) antibody produced in rabbit (Sigma-Aldrich) and a monoclonal anti-myosin light chain antibody produced in mouse (Sigma-Aldrich).

# RESULTS AND DISCUSSION

## Loss of filamin A leads to softer and more fluid-like cells

To investigate the contribution of filamin A to the viscoelastic material properties of cells, we compare two human melanoma cell lines that differ in their expression of filamin A. The M2 cells are filamin A deficient, and the A7 cells are derived from the M2 cells but stably express roughly physiological levels of filamin A (21). The M2 and A7 cells have been used extensively as a comparison for cells with and without filamin A protein. Observations in filamin A-deficient humans (35), knockout mice (36), and knockdown nonmalignant cells (37) provide results consistent with findings in the M2 and A7 cell lines. Lack of filamin A in the M2 cells impairs stability of cell surfaces and translational locomotion,

which are restored in the A7 cells (21). These defects have been suggested, but thus far not confirmed, to result from altered cell mechanics in the absence of filamin A.

Here, we measure the deformation of individual A7 and M2 cells in response to forces applied through a magnetic bead bound to integrins on the cell surface, a technique called MTC (2). To report the mechanical response in terms of the viscoelastic moduli, $G'$ and $G''$, we also measure the bead-cell contact geometry by confocal fluorescence microscopy (see Materials and Methods section). This allows us to account for possible differences between bead embedding in the M2 and A7 cells. To account for possible variations due to cell shape and cytoskeletal organization, we make measurements at two time points: first when they just attach to the substrate and are still round, and 1 day later when they have spread significantly on the substrate.

When plated on rigid, uncoated glass substrates and measured at 2 h post plating, the A7 and M2 cells are both round in shape, with typical heights of 10–15 $\mu$m and few actin bundles visible when stained with fluorescent phalloidin (Fig. 1 *B*). Both the A7 and M2 cells are soft, solid-like materials with an elastic modulus, $G'(\omega) \approx 100$ Pa, that dominates the viscous modulus, $G''(\omega)$, over a broad frequency range. The A7 cells are more solid-like and ~2 times stiffer than the M2 cells (Fig. 1 *C*).

Later, at 24 h, the A7 cells spread out strongly with a typical height of ~5 $\mu$m, a more organized actin cytoskeleton, and visible stress fibers when stained with fluorescent phalloidin (Fig. 1 *B*). The M2 cells spread less strongly and are still somewhat round in shape, with a typical height of ~8 $\mu$m and a less well organized actin cytoskeleton (Fig. 1 *B*). Both cell lines are still soft, solid-like materials over a broad frequency range (Fig. 1 *A*), but now each cell line is stiffer and more solid-like than it was at the earlier time point, consistent with a correlation between spreading and stiffness observed in fibroblasts (38). The A7 cells are two times stiffer than the M2 cells with $|G^*| = 350 \pm 30$ Pa and $|G^*| = 170 \pm 20$ Pa, respectively, and significantly more solid-like with $G''/G' = 0.28 \pm 0.01$ and $G''/G' = 0.36 \pm 0.02$, respectively (Fig. 1 *C*). The fact that the M2 cells are softer and more fluid-like than the A7 cells at both time points suggests that differences in cell shape alone do not account for the observed differences in material properties. These results establish that filamin A does contribute to stiffer and more solid-like cells.

## Loss of filamin A decreases contractile stresses generated by cells

In some types of cells, increased stiffness is associated with increased internal contractile tension (12). Cell contractility arises from internal myosin-generated cytoskeletal tension and is necessary for adherent cells to probe their local mechanical environment in important biological processes such as differentiation, migration, and wound healing, or in disease states such as cancer (7,39–41). To investigate possible mechanisms by which filamin A deficiency leads to decreased cell stiffness, we measure the contractility of the A7 and M2 cells.

We plate cells on deformable polyacrylamide gels that are coated with collagen I. The gels are of physiological stiffness, having a Young's modulus of $E = 1.3$ kPa. Contractile forces generated by the cells are transmitted to the underlying substrate and can be measured using TFM (11,30,42). The A7 cells are strongly contractile and significantly deform the substrate, as shown in Fig. 2 *C*. The M2 cells are much less contractile and only modestly deform the substrate, as shown in Fig. 2 *B*. The net contractile moment, $M$, is a measure of the total strength of the cell contraction against the substrate. The A7 cells have a mean contractile moment of $M = 4.5$ pNm (Fig. 1 *A*). This corresponds to a typical prestress supported by the cytoskeleton of ~600 Pa. The contractile moment for the M2 cells is nearly 10 times less, corresponding to a prestress of ~100 Pa. These data show that M2 cells are indeed less contractile than the A7 cells on collagen I-coated substrates. We hypothesize that the decreased cytoskeletal tension accounts for the decreased stiffness of the M2 cells.

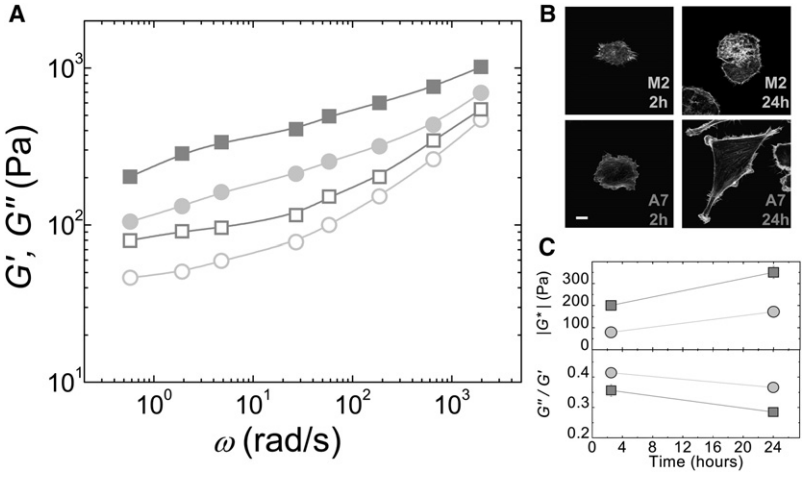


FIGURE 1 Viscoelastic material properties of M2 and A7 melanoma cells cultured on rigid glass substrates. (*A*) Elastic, $G'(\omega)$ (*closed*), and viscous, $G''(\omega)$ (*open*), moduli for A7 (*squares*) and M2 (*circles*) cells cultured for 24 h, as measured by MTC. (*B*) Confocal images of actin cytoskeleton at the basal surface of cells fixed at various times after plating. Bar = 10 $\mu$m. (*C*) Cell stiffness (geometric mean ± SE) measured at $\omega = 5$ rad/s as a function of time after plating; similar time evolution observed for all $\omega$ (*top*). Ratio of viscous to elastic moduli (mean ± SE) of cells as a function of time after plating (*bottom*). Error bars, if not visible, are smaller than the points in this plot.

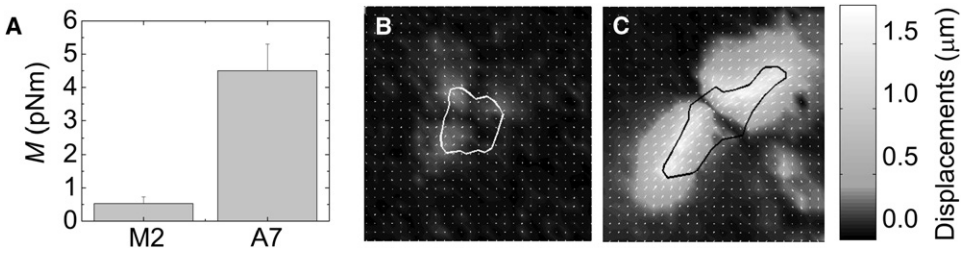


FIGURE 2 Contractile stresses exerted by M2 and A7 cells on collagen I-coated $E = 1.3$ kPa polyacrylamide substrates. (*A*) Mean contractile moment *M*. Examples of contractile deformations induced in the substrate by typical M2 (*B*) and A7 (*C*) cells. Image size, 100 $\mu$m.

## Loss of filamin A impairs cell response to substrate stiffness

In some cells, contractility increases with substrate rigidity, allowing the cell to tune its own stiffness to roughly match that of the substrate, up to some saturation value (43). To further investigate the role of filamin A in the connection between cell stiffness and internal cytoskeletal tension, we plate the M2 and A7 cells on polyacrylamide gels with a range of physiological stiffness values.

On the softest substrates, with $E = 0.1$ kPa, both A7 and M2 cells are weakly spread and round (Fig. 3, *D* and *G*). They have few if any actin bundles that are visible when F-actin is stained with fluorescent phalloidin (data not shown). As the substrate stiffness increases above this, the A7 cells begin to spread and polarize (Fig. 3, *G–I*). They develop contractile stress fibers that are visible when stained with fluorescent phalloidin, similar to those shown in the bottom right corner of Fig. 1 *B*. The M2 cells show a weaker spreading response as substrate stiffness increases (Fig. 3, *D–F*), and never form organized stress fibers (data not shown). To quantify spreading, the mean projected cell area is plotted as a function of substrate stiffness in Fig. 3 *C*. As the substrate stiffness is increased from soft 0.1 kPa to stiff 24 kPa substrates, the mean A7 cell area increases more strongly than the M2 cell area.

These findings are consistent with recent reports that filamin A plays a key role in early cell spreading events. It is recruited to the cortex during early spreading, and loss of filamin A reduces the number of cell extensions (37,44). Although filamin A's role in spreading is not well understood, it is known that, in addition to cross-linking F-actin, filamin A binds a number of important signaling and adhesion molecules, including Rho GTPases, Rho GTPase

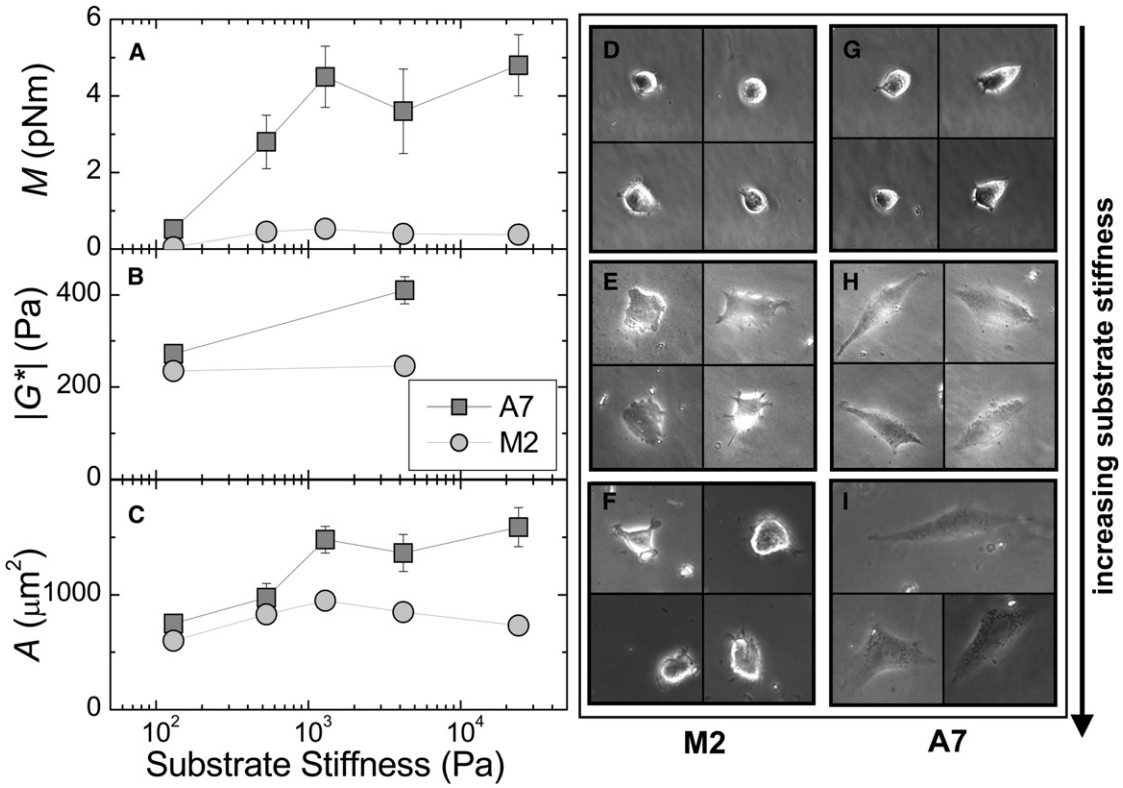


FIGURE 3 Contractility, stiffness, and spreading of M2 and A7 cells grown on collagen I-coated polyacrylamide substrates of increasing stiffness. (*A*) Cell contractile moment (mean ± SE). (*B*) Cell stiffness (geometric mean ± SE). (*C*) Projected cell area (mean ± SE). (*D–I*) Examples of cells grown on $E = 0.1$, 1.3, and 24 kPa substrates.

regulators, and $\beta$ integrins (45,46), making filamin A an attractive candidate for involvement in cytoskeletal remodeling and cell spreading.

On the softest substrates, the M2 cells are very weakly contractile, with a contractile moment of ~0.1 pNm, as shown in Fig. 3 *A*. The A7 cells are somewhat more contractile, with $M = 0.5$ pNm. As the substrate stiffness is increased, the A7 cells show a strong, significant increase in contractility, reaching a maximum of $M = 5$ pNm. The contractile behavior of the A7 cells is consistent with previous studies that revealed a strong correlation between cell contractility and substrate stiffness (27,40,47). In contrast, the M2 cells are weakly contractile, with contractile moments that are never more than 0.5 pNm and are nearly independent of substrate stiffness.

We are not aware of direct interactions between filamin A and myosin II that would directly alter contractility; however, motors and cross-linking proteins may influence each other by more indirect mechanisms, as suggested previously (48). For example, tension exerted on the actin filament by the motor could affect binding of other proteins, or organization of the F-actin network microstructure by one protein could accommodate (or not) binding of the other protein.

To confirm that cell stiffness is indeed correlated with internal contractile tension, we use MTC to probe the material properties of cells grown on the same substrates. On the softest substrates, the A7 and M2 cells have similar stiffness values of ~250 Pa (Fig. 3 *B*). As substrate stiffness is increased to 4 kPa, the A7 cells stiffen significantly to nearly $|G^*| = 400$ Pa; the M2 cell stiffness does not show any response to substrate stiffness.

To summarize, on the softest gels, A7 and M2 cells are soft and only very weakly contractile. As substrate stiffness is increased, the A7 cells respond with increased contractility and an associated increase in stiffness, consistent with previous findings that cell stiffness increases linearly with contractility (12). In contrast, the M2 cells show smaller changes in contractility and do not stiffen as the substrate stiffness is varied over many orders of magnitude. The lack of substrate rigidity response in M2 cells on collagen-coated substrates suggests that filamin A is essential for the active processes underlying this response. We hypothesize that, as in the reconstituted actin-filamin-myosin networks, filamin A is required for the buildup of internal myosin-generated tension in the actin cytoskeleton. However, within the cell, filamin A may mediate contractile tension buildup and stiffening directly through cross-linking (as in the reconstituted networks) or by promoting cell adhesion and spreading via integrin binding (Fig. 4 *A*).

## The stiffness of A7 cells, but not of M2 cells, is strongly decreased by blebbistatin

To test the hypothesis that filamin A is required for the buildup of internal myosin-generated tension in the cytoskeleton, we first confirm the role of myosin-generated cytoskeletal tension in tuning cell stiffness. We measure the material properties of cells that have been treated with blebbistatin, an inhibitor of myosin II ATPase activity (26). Treatment with 50 $\mu$M blebbistatin for 20 min slightly increases the fluid-like nature of both cell lines (Fig. 4 *B*, *bottom*). The A7 cells treated with blebbistatin have a significant decrease in stiffness of 64% compared to control cells (Fig. 4 *B*, *top*). This behavior is consistent with the picture that cells tune their own stiffness with acto-myosin-generated tension, which has been observed in other cells (8,12). In marked contrast, blebbistatin-treated M2 cells show a much smaller decrease in stiffness of only 14% compared to control cells. Since the M2 cells are at a low level of internal stress to begin with, myosin inhibition can only modestly decrease their stiffness, consistent with a lower stiffness compared to A7 cells in the absence of blebbistatin (Fig. 1). This suggests that the stiffness of the M2 cells may be dominated by the linear elastic properties of the intracellular biopolymer network, rather than being actively tuned by acto-myosin-generated tension.

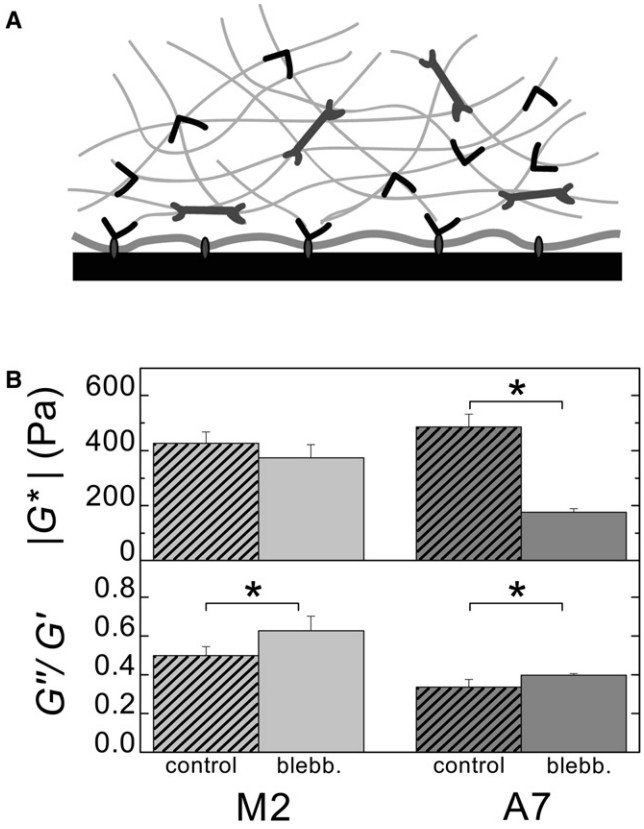


FIGURE 4 (*A*) Schematic showing various roles for filamin A in cell mechanics. Filamin A cross-links actin filaments into orthogonal networks, which support contractile stresses generated by myosin II, and also binds some integrins, linking the actin cytoskeleton to the cell membrane. (*B*) Effect of myosin II inhibition on material properties of A7 and M2 cells. Cell stiffness (geometric mean ± SE) and the ratio of viscous to elastic moduli (mean ± SE) for control cells and cells treated with 50 $\mu$M blebbistatin for 20 min. * indicates that $p < 0.05$.

### M2 and A7 cells have similar levels of phosphorylated myosin II light chain

To discount the possibility that the M2 cells have a lower level of active myosin II, which could account for their decreased contractility and stiffness, we measure the levels of phosphorylated myosin II light chain (pMLC) and myosin II light chain (MLC) in the A7 and M2 cells by Western blotting. We find similar levels of pMLC between the M2 and A7 cells, as shown in Fig. 5 *A*. The pMLC levels can be decreased in a dose-dependent fashion by treatment with the Rho-associated kinase inhibitor Y-27632 (Fig. 5 *A*). The contractility of the A7 cells is strongly decreased by treatment with 10 $\mu$M Y-27632, whereas the contractility of the M2 cells is not measurably affected (Fig. 5 *B*). This is consistent with the very low level of M2 contractility to begin with. These data demonstrate that even though the M2 and A7 cells have similar levels of pMLC, the tensions that build up in the two cells are drastically different. This supports the hypothesis that the defect in the filamin A-deficient M2 cells is in the buildup of internal tension, not in the potential for production of that tension by myosin II.

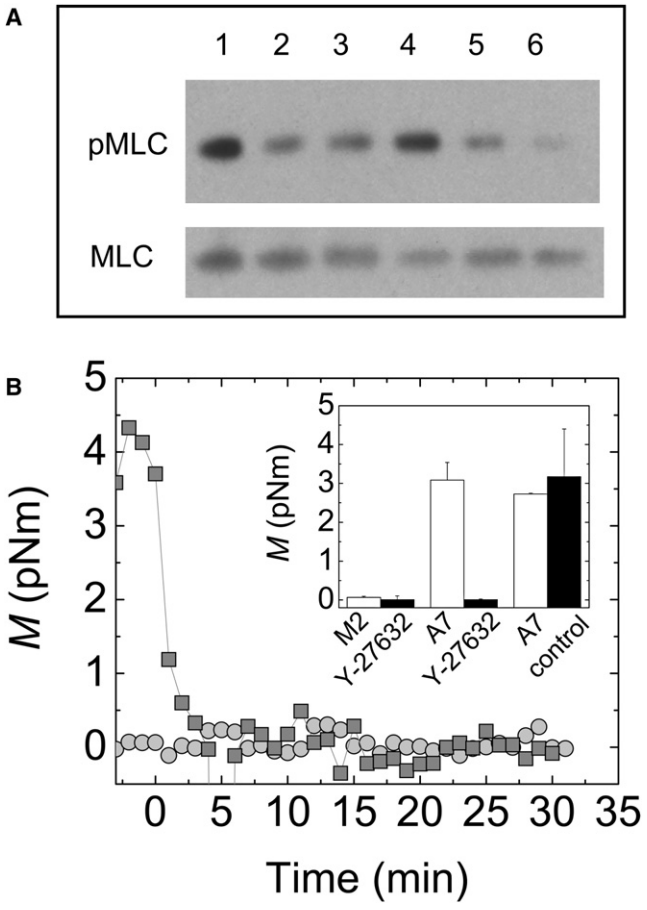


FIGURE 5 (*A*) Western blots showing similar levels of pMLC and MLC in M2 (*lanes 1–3*) and A7 (*lanes 4–6*) cells plated on collagen I. pMLC levels are decreased in a dose-dependent manner by treatment with 0 $\mu$M (*lanes 1* and *4*), 10 $\mu$M (*lanes 2* and *5*), or 50 $\mu$M (*lanes 3* and *6*) of the Rho-associated kinase inhibitor Y-27632. (*B*) Contractile moment, *M*, of a single M2 (*circles*) or A7 (*squares*) cell after addition of 10 $\mu$M Y-27632 to the media at $t = 0$. (*Inset*) Contractile moment (mean $\pm$ SE) for cells before (*white*) and after (*black*) 20 min of treatment with either 10 $\mu$M Y-27632 or control media.

### Role of filamin A in adhesion

In addition to being an efficient cross-linker of F-actin, filamin A also binds the cytoplasmic tail of $\beta$1 integrin, a receptor for collagen I, linking the actin cytoskeleton and cell membrane. Thus, loss of filamin A could potentially impact the ability of cells to adhere strongly to collagen-coated substrates. If adhesion is prevented in the M2 cells, this might account for the low tension and stiffness, in a manner analogous to poor boundary adhesion in the in vitro actin-filamin-myosin system. To dissect the possible mechanisms by which filamin A could promote the buildup of internal cytoskeletal tension within the cell, we measure the adhesion of the M2 and A7 cells to collagen I-coated glass. Cells are plated sparsely on round coated coverslips and grown for 24 h before exposure to fluid shear stresses imposed by the spinning disk method (34). Shear stresses on the apical surface of cells increase linearly with distance, *r*, from the center of the coverslip.

After exposure to fluid shear stresses, the fraction of A7 cells still bound to the substrate decreases with *r*, reaching half of its $r = 0$ value at $r = 3.1$ mm (Fig. 6). The density of bound M2 cells falls off more quickly, reaching half its $r = 0$ value at $r = 1.8$ mm. Thus, the mean adhesion strength of the M2 cells is ~58% that of the A7 cells (Fig. 6, *inset*). The difference in adhesion strength between the cells corresponds well to the difference in projected area between them.

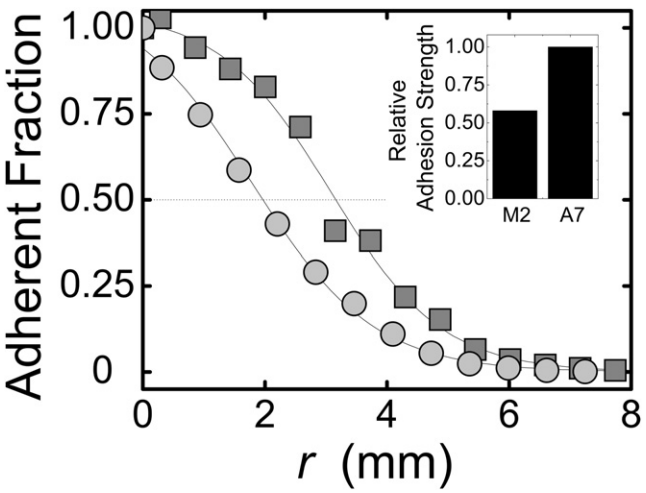


FIGURE 6 Adhesion strength of M2 (*circles*) and A7 (*squares*) cells to collagen I-coated substrates, measured by the spinning disk method (34). After cells are exposed to fluid shear stress, adherent fraction is measured as a function of distance *r* from the center of the coverslip. Shear stresses on apical surface of cells increase linearly with *r*. (*Inset*) Relative adhesion strength determined from radius at which 50% of cells have detached.

Additionally, the rounder and taller M2 cells may experience greater stresses than the A7 cells at equivalent radii, simply due to shape. Our results, then, may reflect a difference in adhesion or in cell shape.

Although loss of filamin A in the M2 cells diminishes the strength of adhesion to collagen I substrates, it does not wholly prevent it. Indeed, adhesion strength is not diminished by the absence of filamin A as strongly as the contractile stresses exerted by the cell on the substrate. Taken together, these data suggest that although decreased adhesion strength may contribute in part to the inability of M2 cells to build up large internal cytoskeletal tensions, it alone does not account for the effect. In fact, decreased cytoskeletal tension could lead to the decreased adhesion and spreading of the M2 cells.

The binding of filamin A to $\beta$1 integrin may also affect the active cell spreading and cytoskeletal reorganization responses downstream of integrin engagement and activation, which will affect the buildup of internal tension and stiffening. We do not directly investigate this mechanism by which filamin A might be essential to the cell stiffening response, but it is currently being explored by other investigators (32).

## Role of filamin A in cells subjected to large external stresses

To test whether filamin A is required for stiffening of cells exposed to large *external* stresses, we use magnetic tweezers to pull with 0.5–10 nN forces on fibronectin-coated beads that are attached to individual M2 or A7 cells (33), and observe the resulting cell deformation. From these experiments, we measure the cell's nonlinear elasticity.

More than 95% of beads stay bound to the A7 cells, up to the maximum 10 nN loading force, as shown in the inset to Fig. 7 *A*. In contrast, beads are disrupted from M2 cells at forces of $<$1 nN, and $>$25% of beads are disrupted at 10 nN. This increase in bead binding strength to the A7 cells is consistent with two possible roles for filamin A: increased bead-cell adhesion, or increased stress supported by the cortical actin network before rupture.

At the lowest 0.5–1 nN forces, the A7 cells are 2–3 times stiffer than the M2 cells (Fig. 7 *A*). This stiffness is essentially the ratio of the force to the displacement and depends on the bead-cell geometry. We can estimate the typical deformation or strain, $\gamma$, as the bead displacement $d$ divided by the bead radius $R$, and the typical stress, $\sigma$, as the applied force divided by the bead cross-sectional area. For the smallest 0.5 nN load, $\sigma$ ~30 Pa, yielding estimated moduli of 300 Pa and 150 Pa for the A7 and M2 cells, respectively (Fig. 7 *A*), in agreement with the moduli determined by MTC (Fig. 1).

Although the A7 cells start out stiffer than the M2 cells, both stiffen strongly as increasing loads are applied (Fig. 7 *A*). Between 0.5 and 10 nN, the stiffness of both cell types increases by 3–4 nN/$\mu$m, a threefold increase for the A7 cells and a fourfold increase for the M2 cells. There is no significant difference in the form of the nonlinearity between the two cell types. Thus, we find that filamin A is, in fact, not required for the passive stiffening of cells under large external stress.

For the maximum 10 nN load, we estimate $\sigma \sim 600$ Pa and $\gamma \sim 0.7$–1. In vitro experiments suggest that F-actin cross-linked by filamin A would support and significantly stiffen under these strains (16), whereas F-actin cross-linked by more rigid proteins would rupture (15). In addition, reconstituted gels of the intermediate filament vimentin, a biopolymer that is expressed in the M2 and A7 cells, also can support and stiffen under these large deformations (49). It would be an interesting design feature if the cell used two complementary cytoskeletal networks for tuning cell stiffness: 1), the actin network for active tuning of cell stiffness in response to stimuli; and 2), the intermediate filament network for a passive, but very fast, stiffening response to potentially damaging large external forces. Indeed, when we treat M2 and A7 cells with 5 $\mu$M cytochalasin-D, a drug that disrupts the actin cytoskeleton, the cells are softened significantly but the nonlinear stiffening is not abolished, as shown in Fig. 7 *B*. In fact, the overall magnitude and shape of the nonlinear stiffening response in both cell types are unchanged by cytochalasin-D. To elucidate the physical and molecular origins of nonlinear stiffening under external stress, the contribution of other actin cross-linking proteins, including other filamin

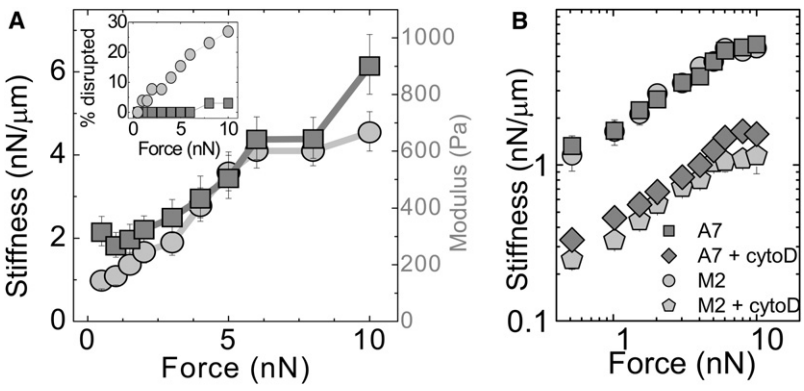


FIGURE 7 Stiffening of A7 and M2 cells subjected to large nanonewton-scale external forces, applied by magnetic tweezers through a fibronectin-coated magnetic bead. (*A*) Cell stiffness and estimated modulus (geometric mean $\pm$ SE) as a function of force for A7 (*squares*, $n = 30$) and M2 (*circles*, $n = 19$) cells. (*Inset*) Percentage of beads disrupted from cells as a function of force. (*B*) Cell stiffness as a function of force for A7 ($n = 9$) and M2 ($n = 7$) cells treated with 5 $\mu$M cytochalasin-D for 15 min.

isoforms, and the intermediate filament network should be investigated in future work.

## CONCLUSIONS

We have demonstrated that filamin A plays a key role in the ability of subconfluent cells grown on collagen-coated substrates to actively tune their own stiffness. The filamin A-deficient M2 cells are soft and exert extremely low levels of contractile stresses against the substratum, regardless of mechanical environment. These properties are nearly unchanged by inhibition of myosin II with drugs. In contrast, the filamin A-replete A7 cells are stiffer and more contractile, and can actively tune their properties in response to changes in substrate rigidity. The stiffness and contractility of the A7 cells are significantly diminished by myosin II inhibitors.

These results are consistent with the hypothesis that filamin A is required for buildup of the large *internal* cytoskeletal tensions that stiffen the cell. This hypothesis was motivated by an in vitro reconstituted cytoskeletal system in which cross-linking of F-actin by filamin A is necessary for forces, generated by assemblies of myosin II, to build up and stiffen the network instead of relaxing away. It seems that in the cell, filamin A is also required for the buildup of myosin-generated tension, but the mechanism is very likely more complex. In addition to cross-linking F-actin in the cortex, filamin A also binds integrins, which affect cell contractility, spreading, and adhesion. Indeed, loss of filamin A diminishes all of these. This key role for filamin A will have implications for different models of cell material properties and mechanotransduction.

Surprisingly, we find that filamin A is not required for the passive stiffening of cells deformed by large *external* forces. It could be that the loss of filamin's F-actin cross-linking can be compensated for by other actin cross-linkers. It is also possible that the actin cytoskeleton is not responsible for the mechanical response to large external forces in vivo. Intermediate filament networks have long been thought to be responsible for the stability of cells because they can support large strains before breaking. Indeed, reconstituted vimentin networks also can support large deformations and stiffen significantly with externally applied stress (49). It would be an interesting design feature for the cell to employ two different cytoskeletal systems for two different types of stiffening responses. The stiffness of the actin cytoskeleton can be actively tuned by myosin-generated stresses in response to mechanical and chemical cues. The intermediate filaments, which can withstand large strains but lack motor proteins to internally prestress them, stiffen passively to stabilize the cell in response to large external forces. This hypothesis could be tested in vivo by investigating the contribution of the different cytoskeletal systems to the nonlinear elasticity of cells, or in vitro by investigating the nonlinear elasticity of composite networks of actin-filamin-myosin and intermediate filaments.

We thank M. L. Gardel and P. A. Janmey for many helpful discussions.

This work was supported by the National Science Foundation (DMR-0602684 and CTS-0505929) and the Harvard Materials Research Science and Engineering Center (DMR-0820484). D.A.W., F.N., and T.P.S. were supported by the HUSEC Seed Fund for Interdisciplinary Science. T.P.S. and N.W. were supported by grants from the National Institutes of Health (HL-19429 and GM07274, respectively). K.E.K. was supported by a National Defense Science and Engineering Graduate Fellowship and a National Science Foundation Graduate Research Fellowship.

## REFERENCES

1. Bausch, A. R., F. Ziemann, A. A. Boulbitch, K. Jacobson, and E. Sackmann. 1998. Local measurements of viscoelastic parameters of adherent cell surfaces by magnetic bead microrheometry. *Biophys. J.* 75:2038–2049.
2. Fabry, B., G. N. Maksym, J. P. Butler, M. Glogauer, D. Navajas, et al. 2001. Scaling the microrheology of living cells. *Phys. Rev. Lett.* 87:148102.
3. Hoffman, B. D., G. Massiera, K. M. Van Citters, and J. C. Crocker. 2006. The consensus mechanics of cultured mammalian cells. *Proc. Natl. Acad. Sci. USA.* 103:10259–10264.
4. Radmacher, M., M. Fritz, C. M. Kacher, J. P. Cleveland, and P. K. Hansma. 1996. Measuring the viscoelastic properties of human platelets with the atomic force microscope. *Biophys. J.* 70:556–567.
5. Na, S., O. Collin, F. Chowdhury, B. Tay, M. Ouyang, et al. 2008. Rapid signal transduction in living cells is a unique feature of mechanotransduction. *Proc. Natl. Acad. Sci. USA.* 105:6626–6631.
6. Sawada, Y., M. Tamada, B. J. Dubin-Thaler, O. Cherniavskaya, R. Sakai, et al. 2006. Force sensing by mechanical extension of the Src family kinase substrate p130Cas. *Cell.* 127:1015–1026.
7. Discher, D. E., P. Janmey, and Y. L. Wang. 2005. Tissue cells feel and respond to the stiffness of their substrate. *Science.* 310:1139–1143.
8. Fernandez, P., P. A. Pullarkat, and A. Ott. 2006. A master relation defines the nonlinear viscoelasticity of single fibroblasts. *Biophys. J.* 90:3796–3805.
9. Wang, N., J. P. Butler, and D. E. Ingber. 1993. Mechanotransduction across the cell surface and through the cytoskeleton. *Science.* 260:1124–1127.
10. Harris, A. K., P. Wild, and D. Stopak. 1980. Silicone rubber substrata: a new wrinkle in the study of cell locomotion. *Science.* 208:177–179.
11. Pelham, Jr., R. J., and Y. Wang. 1999. High resolution detection of mechanical forces exerted by locomoting fibroblasts on the substrate. *Mol. Biol. Cell.* 10:935–945.
12. Wang, N., I. M. Tolic-Norrelykke, J. Chen, S. M. Mijailovich, J. P. Butler, et al. 2002. Cell prestress. I. Stiffness and prestress are closely associated in adherent contractile cells. *Am. J. Physiol. Cell Physiol.* 282:C606–C616.
13. Bausch, A. R., and K. Kroy. 2006. A bottom-up approach to cell mechanics. *Nat. Phys.* 2:231–238.
14. Mohrdieck, C., F. Dalmas, E. Arzt, R. Tharmann, M. M. Claessens, et al. 2007. Biomimetic models of the actin cytoskeleton. *Small.* 3:1015–1022.
15. Gardel, M. L., J. H. Shin, F. C. MacKintosh, L. Mahadevan, P. Matsudaira, et al. 2004. Elastic behavior of cross-linked and bundled actin networks. *Science.* 304:1301–1305.
16. Gardel, M. L., F. Nakamura, J. H. Hartwig, J. C. Crocker, T. P. Stossel, et al. 2006. Prestressed F-actin networks cross-linked by hinged filamins replicate mechanical properties of cells. *Proc. Natl. Acad. Sci. USA.* 103:1762–1767.
17. Wagner, B., R. Tharmann, I. Haase, M. Fischer, and A. R. Bausch. 2006. Cytoskeletal polymer networks: the molecular structure of cross-linkers determines macroscopic properties. *Proc. Natl. Acad. Sci. USA.* 103:13974–13978.

18. Flanagan, L. A., J. Chou, H. Falet, R. Neujahr, J. H. Hartwig, et al. 2001. Filamin A, the Arp2/3 complex, and the morphology and function of cortical actin filaments in human melanoma cells. *J. Cell Biol.* 155:511–517.

19. Kiema, T., Y. Lad, P. Jiang, C. L. Oxley, M. Baldassarre, et al. 2006. The molecular basis of filamin binding to integrins and competition with talin. *Mol. Cell.* 21:337–347.

20. Calderwood, D. A., A. Huttenlocher, W. B. Kiosses, D. M. Rose, D. G. Woodside, et al. 2001. Increased filamin binding to beta-integrin cytoplasmic domains inhibits cell migration. *Nat. Cell Biol.* 3:1060–1068.

21. Cunningham, C. C., J. B. Gorlin, D. J. Kwiatkowski, J. H. Hartwig, P. A. Janmey, et al. 1992. Actin-binding protein requirement for cortical stability and efficient locomotion. *Science.* 255:325–327.

22. Glogauer, M., P. Arora, D. Chou, P. A. Janmey, G. P. Downey, et al. 1998. The role of actin-binding protein 280 in integrin-dependent mechanoprotection. *J. Biol. Chem.* 273:1689–1698.

23. Kainulainen, T., A. Pender, M. D'Addario, Y. Feng, P. Lekic, et al. 2002. Cell death and mechanoprotection by filamin A in connective tissues after challenge by applied tensile forces. *J. Biol. Chem.* 277:21998–22009.

24. Tandon, R., I. Levental, C. Huang, F. J. Byfield, J. Ziembicki, et al. 2007. HIV infection changes glomerular podocyte cytoskeletal composition and results in distinct cellular mechanical properties. *Am. J. Physiol. Renal Physiol.* 292:F701–F710.

25. Coughlin, M. F., M. Puig-de-Morales, P. Bursac, M. Mellema, E. Millet, et al. 2006. Filamin-A and rheological properties of cultured melanoma cells. *Biophys. J.* 90:2199–2205.

26. Straight, A. F., A. Cheung, J. Limouze, I. Chen, N. J. Westwood, et al. 2003. Dissecting temporal and spatial control of cytokinesis with a myosin II Inhibitor. *Science.* 299:1743–1747.

27. Pelham, Jr., R. J., and Y. Wang. 1997. Cell locomotion and focal adhesions are regulated by substrate flexibility. *Proc. Natl. Acad. Sci. USA.* 94:13661–13665.

28. Engler, A., L. Bacakova, C. Newman, A. Hategan, M. Griffin, et al. 2004. Substrate compliance versus ligand density in cell on gel responses. *Biophys. J.* 86:617–628.

29. Butler, J. P., I. M. Tolic-Norrelykke, B. Fabry, and J. J. Fredberg. 2002. Traction fields, moments, and strain energy that cells exert on their surroundings. *Am. J. Physiol. Cell Physiol.* 282:C595–C605.

30. Tolic-Norrelykke, I. M., J. P. Butler, J. Chen, and N. Wang. 2002. Spatial and temporal traction response in human airway smooth muscle cells. *Am. J. Physiol. Cell Physiol.* 283:C1254–C1266.

31. Mijailovich, S. M., M. Kojic, M. Zivkovic, B. Fabry, and J. J. Fredberg. 2002. A finite element model of cell deformation during magnetic bead twisting. *J. Appl. Physiol.* 93:1429–1436.

32. Byfield, F. J., Q. Wen, I. Levental, K. Nordstrom, P. E. Arratia, et al. 2009. Absence of filamin A prevents cells from responding to stiffness gradients on gels coated with collagen but not fibronectin. *Biophys. J.* In press.

33. Mierke, C. T., P. Kollmannsberger, D. P. Zitterbart, J. Smith, B. Fabry, et al. 2008. Mechano-coupling and regulation of contractility by the vinculin tail domain. *Biophys. J.* 94:661–670.

34. Boettiger, D. 2007. Quantitative measurements of integrin-mediated adhesion to extracellular matrix. *Methods Enzymol.* 426:1–25.

35. Fox, J. W., and C. A. Walsh. 1999. Periventricular heterotopia and the genetics of neuronal migration in the cerebral cortex. *Am. J. Hum. Genet.* 65:19–24.

36. Feng, Y., M. H. Chen, I. P. Moskowitz, A. M. Mendonza, L. Vidali, et al. 2006. Filamin A (FLNA) is required for cell-cell contact in vascular development and cardiac morphogenesis. *Proc. Natl. Acad. Sci. USA.* 103:19836–19841.

37. Kim, H., A. Sengupta, M. Glogauer, and C. A. McCulloch. 2008. Filamin A regulates cell spreading and survival via $\beta$1 integrins. *Exp. Cell Res.* 314:834–846.

38. Thoumine, O., O. Cardoso, and J. J. Meister. 1999. Changes in the mechanical properties of fibroblasts during spreading: a micromanipulation study. *Eur. Biophys. J.* 28:222–234.

39. Cai, S., L. Pestic-Dragovich, M. E. O'Donnell, N. Wang, D. Ingber, et al. 1998. Regulation of cytoskeletal mechanics and cell growth by myosin light chain phosphorylation. *Am. J. Physiol.* 275:C1349–C1356.

40. Engler, A. J., S. Sen, H. L. Sweeney, and D. E. Discher. 2006. Matrix elasticity directs stem cell lineage specification. *Cell.* 126:677–689.

41. Paszek, M. J., N. Zahir, K. R. Johnson, J. N. Lakins, G. I. Rozenberg, et al. 2005. Tensional homeostasis and the malignant phenotype. *Cancer Cell.* 8:241–254.

42. Dembo, M., and Y. L. Wang. 1999. Stresses at the cell-to-substrate interface during locomotion of fibroblasts. *Biophys. J.* 76:2307–2316.

43. Solon, J., I. Levental, K. Sengupta, P. C. Georges, and P. A. Janmey. 2007. Fibroblast adaptation and stiffness matching to soft elastic substrates. *Biophys. J.* 93:4453–4461.

44. Mammoto, A., S. Huang, and D. E. Ingber. 2007. Filamin links cell shape and cytoskeletal structure to Rho regulation by controlling accumulation of p190RhoGAP in lipid rafts. *J. Cell Sci.* 120:456–467.

45. Stossel, T. P., J. Condeelis, L. Cooley, J. H. Hartwig, A. Noegel, et al. 2001. Filamins as integrators of cell mechanics and signalling. *Nat. Rev. Mol. Cell Biol.* 2:138–145.

46. Stossel, T. P., and J. H. Hartwig. 2003. Filling gaps in signaling to actin cytoskeletal remodeling. *Dev. Cell.* 4:444–445.

47. Polte, T. R., G. S. Eichler, N. Wang, and D. E. Ingber. 2004. Extracellular matrix controls myosin light chain phosphorylation and cell contractility through modulation of cell shape and cytoskeletal prestress. *Am. J. Physiol. Cell Physiol.* 286:C518–C528.

48. Reichl, E. M., Y. Ren, M. K. Morphew, M. Delannoy, J. C. Effler, et al. 2008. Interactions between myosin and actin crosslinkers control cytokinesis contractility dynamics and mechanics. *Curr. Biol.* 18:471–480.

49. Janmey, P. A., U. Euteneuer, P. Traub, and M. Schliwa. 1991. Viscoelastic properties of vimentin compared with other filamentous biopolymer networks. *J. Cell Biol.* 113:155–160.